

Stability and Turing Patterns of a Predator-prey Model with Holling Type II Functional Response and Allee Effect in Predator

Lu CHEN, Feng YANG, Yong-li SONG[†]

School of Mathematics, Hangzhou Normal University, Hangzhou 311121, China
([†]E-mail: songyl@hznu.edu.cn)

Abstract In this paper, we are concerned with a predator-prey model with Holling type II functional response and Allee effect in predator. We first mathematically explore how the Allee effect affects the existence and stability of the positive equilibrium for the system without diffusion. The explicit dependent condition of the existence of the positive equilibrium on the strength of Allee effect is determined. It has been shown that there exist two positive equilibria for some modulate strength of Allee effect. The influence of the strength of the Allee effect on the stability of the coexistence equilibrium corresponding to high predator biomass is completely investigated and the analytically critical values of Hopf bifurcations are theoretically determined. We have shown that there exists stability switches induced by Allee effect. Finally, the diffusion-driven Turing instability, which can not occur for the original system without Allee effect in predator, is explored, and it has been shown that there exists diffusion-driven Turing instability for the case when predator spread slower than prey because of the existence of Allee effect in predator.

Keywords predator-prey model; Allee effect; diffusion; stability; Turing bifurcation

2000 MR Subject Classification 34C60; 37G10; 92D25

1 Introduction

The relationship between predator and prey is one of the most basic and universal relationships among populations in nature. It is the primary ecosystem for maintaining ecological balance, species reproduction, and biodiversity. The qualitative study of the dynamics of the predator-prey system is also one of the base problems in the field of biological mathematics. The classic Rosenzweig-MacArthur predator-prey model is described by the following equations

$$\begin{cases} \frac{du}{dt} = ru\left(1 - \frac{u}{K}\right) - \frac{auv}{1 + bu}, \\ \frac{dv}{dt} = \frac{acv}{1 + bu} - dv, \end{cases} \quad (1.1)$$

where $u(t)$ and $v(t)$ respectively represent the population density of the prey population and predator population at time t ; r is the intra-specific growth rate of the prey population; K represents the maximum environmental capacity; a is the search efficiency of the predator population; b is a positive constant, used to measure the ability of a predator to kill and eat a prey; c is the efficiency of the consumed prey to be converted into predator births; d is the

Manuscript received on February 22, 2021. Accepted on May 10, 2023.

The project is supported by the National Natural Science Foundation of China (No.11971143; 12071105) and Zhejiang Provincial Natural Science Foundation of China (No.LZ23A010001).

[†]Corresponding author.

inherent mortality rate of the predator population. The globally asymptotical stability for the boundary equilibria and the positive equilibrium, Hopf bifurcation and the uniqueness have been investigated in [9, 11]. The stability, Hopf bifurcation and spatiotemporal patterns for the diffusive version of system (1.1) have been considered in [12, 41].

In system (1.1), the prey species follows the logistic growth equation when the predator species is absent. The logistic growth equation shows that the unit growth rate of the population decreases with the increase of population. However, in the case of scarce resources, when the population density is relatively small, the increase of the population density is conducive to reciprocal capture, cooperative foraging, and reproduction. In this case, the unit growth rate of the population increases with the increase of population density, which is called the Allee effect in biology. There is evidence of Allee effects caused by at least six mechanisms: mate limitation, cooperative defense, predator satiation, cooperative feeding, dispersal, and habitat alteration^[17]. And it has been shown that Allee effects are an important dynamic phenomenon in many population evolution processes such as extinction and biological invasion^[1, 5, 13, 14]. There has been recently increasing interest in investigating the potential influence of Allee effects on the dynamics of the single population^[8, 15, 20, 23] and the population systems arising from the fields of biology, ecology and biomathematics^[6, 10, 16, 21, 27, 29–31, 37, 39, 42–44].

For the predator-prey system, Allee effect is often encountered in the prey population and has been widely investigated in the literatures (see, for instance, [2, 19, 21, 22, 24, 27–30, 32, 37, 40, 42, 44] and references therein). But in real life, the predator population is usually much smaller than the prey population, so the predator population is more susceptible to the Allee effect than the prey population^[34]. The size-selective predation, mate-limitation, positive feedbacks of top predators on nutrient cycling, foraging facilitation among predators and strength of hunting cooperation among the predators are considered as the main biological mechanisms for the Allee effect in the predator^[3, 26, 33, 36, 43]. However, compared with the Allee effect in the prey, there are few theoretical studies^[4, 18, 28, 34–36, 38, 43, 45] on the influence of the Allee effect of the predator on dynamics of the predator-prey system .

Zhou et al.^[43] introduced the Allee effect of the predator into the Lotka-Volterra system and have shown that the Allee effect may be a destabilizing force in predator-prey systems. Bodine and Yus^[4] proposed a modified version of the model presented by Zhou et al.^[43] by incorporating both an Allee effect and intraspecific competition into the predator and have shown that there exist biologically reasonable parameter sets which produce a stable coexistence equilibrium. In^[18], Lai et al. replaced the exponential population growth on prey of the model presented by Zhou et al.^[43] by the Logistic growth and have shown that the weak Allee effect can bring rich and complicated dynamics to the previous simple model. The local and global stability of the positive equilibrium and Turing instability for the diffusive Holling-Tanner prey-predator model with the Allee effect in predator have been investigated by Wang et al.^[38]. The rich bifurcation structure of predator-prey model induced by the Allee Effect in the growth of generalist predator has been studied by Sen et al.^[28]. The influence of the Allee effect in the predator on the dynamics of the predator-prey models with Holling type functional responses has been investigated in [34–36]. The predator-prey model with Holling type-II functional response and Allee effect for predator reproduction is described by the following system of ordinary differential equations

$$\begin{cases} \frac{du}{dt} = ru\left(1 - \frac{u}{K}\right) - \frac{auv}{1+bu}, \\ \frac{dv}{dt} = \frac{acuv}{1+bu}\left(\frac{v}{v+h}\right) - dv, \end{cases} \quad (1.2)$$

where the term $\frac{acu}{1+bu}\left(\frac{v}{v+h}\right)$ represents the average reproduction rate of per predator, $\frac{v}{v+h}$ represents the Allee effect in the predator and the parameter $h \geq 0$ is considered as the Allee effect

strength. Existence and stability of the coexistence equilibria of (1.2) is numerically examined in [34–36]. In [34, 36], it has been shown that if one of the coexistence equilibria is stable, it will always be the one corresponding to high predator biomass by numerical method. In [35], it has been shown that the one corresponding to low predator biomass is a saddle by graphical approach. However, how the coexistence equilibria explicitly depends on the Allee effect strength is still not clear and there is no completely theoretical results on the stability of the positive equilibrium corresponding to high predator biomass. In this paper, we focus on these unsolved problems for (1.2) and further consider the following diffusive version of (1.2)

$$\begin{cases} \frac{\partial u}{\partial t} = d_1 \Delta u + ru \left(1 - \frac{u}{K}\right) - \frac{auv}{1 + bu}, \\ \frac{\partial v}{\partial t} = d_2 \Delta v + v \left(\frac{acu}{1 + bu} \left(\frac{v}{v + h}\right) - d\right), \end{cases} \tag{1.3}$$

where $u(x, y, t)$ and $v(x, y, t)$ represent the densities of prey and predator, respectively, at location $(x, y) \in \mathbb{R}^2$ and time t , $d_1 > 0$ and $d_2 > 0$ are the diffusion coefficients of the prey and predator, respectively. The random movement of two species is modeled by Laplacian operator Δ , where $\Delta = \frac{\partial^2}{\partial x^2} + \frac{\partial^2}{\partial y^2}$.

This paper is organized as follows. In Section 2, we mainly investigate how the existence and stability of the positive equilibria of ordinary differential system depend on the Allee effect strength and the existence of Hopf bifurcation induced by the Allee effect strength. Numerical simulations illustrate and verify the obtained theoretical results. In Section 3, we study the diffusion-driven Turing instability and determine the value of the Turing bifurcation value. And spatial patterns induced by the diffusion are numerically investigated. Finally, we summarize our results and give some biological interpretations in Section 4.

2 Stability and Bifurcation Analysis for the Ordinary Differential System

To reduce the number of parameters of (1.3), we introduce the dimensionless variables

$$\tilde{u} = \frac{u}{K}, \quad \tilde{v} = \frac{av}{r}, \quad \tilde{t} = rt,$$

and the dimensionless parameters

$$\tilde{d}_1 = \frac{d_1}{r}, \quad \tilde{d}_2 = \frac{d_2}{r}, \quad \alpha = bK, \quad \beta = \frac{acK}{r}, \quad \gamma = \frac{ah}{r}, \quad \eta = \frac{d}{r}.$$

Then, dropping the tilde for simplification of notations, (1.3) becomes the following non-dimensional form

$$\begin{cases} \frac{\partial u}{\partial t} = d_1 \Delta u + u(1 - u) - \frac{uv}{1 + \alpha u}, \\ \frac{\partial v}{\partial t} = d_2 \Delta v + v \left(\frac{\beta u}{1 + \alpha u} \left(\frac{v}{v + \gamma}\right) - \eta\right). \end{cases} \tag{2.1}$$

Here, γ measures the strength of the Allee effect in predator. When $\gamma = 0$, there is no Allee effect in predator and (2.1) becomes the predator-prey system with Holling type II functional response. It is obvious that the larger the value of γ is, the lower the per reproduction rate of predator is. In this section, we analytically investigate how the strength $\gamma > 0$ of the Allee effect in predator affects the existence and stability of the positive equilibrium.

2.1 Existence and Stability of the Non-negative Equilibria

First, we consider the following model without diffusion terms

$$\begin{cases} \frac{du}{dt} = u(1 - u) - \frac{uv}{1 + \alpha u}, \\ \frac{dv}{dt} = v\left(\frac{\beta u}{1 + \alpha u}\left(\frac{v}{v + \gamma}\right) - \eta\right). \end{cases} \tag{2.2}$$

System (2.2) has a zero equilibrium $E_0 = (0, 0)$ and a boundary equilibrium $E_1 = (1, 0)$. Assuming that $E_*(u_*, v_*)$ is the positive equilibrium of (2.2), then $v_* = (1 - u_*)(1 + \alpha u_*)$ and u_* is the positive root(s) of the following quadratic equation, satisfying $0 < u_* < 1$,

$$(\beta - \alpha\eta)u^2 - (\beta - \alpha\eta + \eta)u + \eta\gamma + \eta = 0. \tag{2.3}$$

By a simple calculation, we have the following results on the existence of the positive equilibrium of system (2.2).

Theorem 2.1. (I) For $0 < \beta \leq (\alpha + 1)\eta$, system (2.2) has no positive equilibrium for any $\gamma \geq 0$.

(II) For $\beta > (\alpha + 1)\eta$, letting

$$Q = (\beta - (\alpha + 1)\eta)^2 - 4\gamma\eta(\beta - \alpha\eta) \tag{2.4}$$

and

$$\gamma_* = \frac{(\beta - (\alpha + 1)\eta)^2}{4\eta(\beta - \alpha\eta)}, \tag{2.5}$$

we have

- (i) when $\gamma = 0$, system (2.2) has one positive equilibrium $E_*^{(0)}(u_*^{(0)}, (1 - u_*^{(0)})(1 + \alpha u_*^{(0)}))$ with $u_*^{(0)} = \frac{\eta}{\beta - \alpha\eta}$;
- (ii) when $0 < \gamma < \gamma_*$, system (2.2) has two positive equilibria $E_*^-(u_*^-, v_*^-)$ and $E_*^+(u_*^+, v_*^+)$, where $v_*^- = (1 - u_*^-)(1 + \alpha u_*^-)$, $v_*^+ = (1 - u_*^+)(1 + \alpha u_*^+)$ and

$$u_*^- = \frac{\beta - \alpha\eta + \eta - \sqrt{Q}}{2(\beta - \alpha\eta)}, \quad u_*^+ = \frac{\beta - \alpha\eta + \eta + \sqrt{Q}}{2(\beta - \alpha\eta)}; \tag{2.6}$$

- (iii) when $\gamma = \gamma_*$, system (2.2) has one positive equilibrium $E_*^{(1)}(u_*^{(1)}, v_*^{(1)})$ with

$$u_*^{(1)} = \frac{\beta - \alpha\eta + \eta}{2(\beta - \alpha\eta)}, \quad v_*^{(1)} = (1 - u_*^{(1)})(1 + \alpha u_*^{(1)}); \tag{2.7}$$

- (iv) when $\gamma > \gamma_*$, system (2.2) has no positive equilibrium.

Remark 2.2. In fact, it is easy to verify that when $\gamma = 0$ (i.e., without Allee effect in predator), the equilibrium $E_*^-(u_*^-, v_*^-)$ becomes $E_*^{(0)}(u_*^{(0)}, (1 - u_*^{(0)})(1 + \alpha u_*^{(0)}))$, and the equilibrium $E_*^+(u_*^+, v_*^+)$ becomes the boundary equilibrium $E_1(1, 0)$.

Remark 2.3. From (2.6), it is easy to show that $u_*^- < u_*^+$ for $\gamma > 0$. By (2.2), we also have $v_* = \frac{\gamma\eta(1+\alpha u_*)}{(\beta-\alpha\eta)u_*-\eta}$. Thus, we have

$$\frac{dv_*}{du_*} = -\frac{\beta\gamma\eta}{((\beta-\alpha\eta)u_*-\eta)^2} < 0,$$

which, together with the fact that $u_*^- < u_*^+$ for $\gamma > 0$, implies that $v_*^- > v_*^+$ for $\gamma > 0$.

Assume that (u_*, v_*) is the equilibrium of system (2.2), then the corresponding characteristic matrix is $A = (a_{ij})_{2 \times 2}$, where

$$\begin{aligned} a_{11} &= 1 - 2u_* - \frac{v_*}{1 + \alpha u_*} + \frac{\alpha u_* v_*}{(1 + \alpha u_*)^2}, & a_{12} &= -\frac{u_*}{1 + \alpha u_*}, \\ a_{21} &= \frac{\beta v_*^2}{(1 + \alpha u_*)^2(\gamma + v_*)}, & a_{22} &= \frac{\beta u_* v_*}{(1 + \alpha u_*)(\gamma + v_*)} - \eta + \frac{\gamma \beta u_* v_*}{(1 + \alpha u_*)(\gamma + v_*)^2}, \end{aligned} \tag{2.8}$$

and the corresponding characteristic equation is

$$\lambda^2 - Tr(A)\lambda + Det(A) = 0, \tag{2.9}$$

where $Tr(A) = a_{11} + a_{22}$, $Det(A) = a_{11}a_{22} - a_{12}a_{21}$.

Theorem 2.4. *The zero equilibrium $E_0(0, 0)$ of system (2.2) is a saddle for $\gamma \geq 0$. For the boundary equilibrium $E_1(1, 0)$ of system (2.2), when $\gamma = 0$, it is a stable node for $\beta < (\alpha + 1)\eta$ and a saddle for $\beta > (\alpha + 1)\eta$; when $\gamma > 0$, it is a stable node for any $\alpha, \beta, \eta > 0$.*

The proof of Theorem 2.4 is simple and we omit it.

If (u_*, v_*) is the positive equilibrium of the system (2.2), then (2.8) becomes

$$\begin{aligned} a_{11} &= -u_* + \frac{\alpha u_* v_*}{(1 + \alpha u_*)^2}, & a_{12} &= -\frac{u_*}{1 + \alpha u_*} < 0, \\ a_{21} &= \frac{\beta v_*^2}{(1 + \alpha u_*)^2(\gamma + v_*)} > 0, & a_{22} &= \frac{\gamma \beta u_* v_*}{(1 + \alpha u_*)(\gamma + v_*)^2} > 0. \end{aligned} \tag{2.10}$$

When $\gamma = 0$, (2.1) becomes the well-known predator-prey system with Holling type II functional response and here we introduce the following results by [9, 11].

Lemma 2.5. *When $\gamma = 0$, the stability of the unique positive equilibrium $E_*^{(0)}(u_*^{(0)}, v_*^{(0)})$ under the condition $\beta > (\alpha + 1)\eta$ is shown as follows*

- (i) *when $0 \leq \alpha \leq 1$, $E_*^{(0)}(u_*^{(0)}, v_*^{(0)})$ is always stable for $\beta > (\alpha + 1)\eta$;*
- (ii) *when $\alpha > 1$, $E_*^{(0)}(u_*^{(0)}, v_*^{(0)})$ is stable for $(\alpha + 1)\eta < \beta < \frac{\alpha}{\alpha-1}(\alpha + 1)\eta$ and unstable for $\beta > \frac{\alpha}{\alpha-1}(\alpha + 1)\eta$, and system (2.2) has a unique limit cycle for $\beta > \frac{\alpha}{\alpha-1}(\alpha + 1)\eta$.*

In the following, we investigate the influence of $\gamma(0 < \gamma \leq \gamma_*)$ on the stability of the positive equilibrium under the assumption that the positive equilibrium $E_*^{(0)}(u_*^{(0)}, v_*^{(0)})$ is stable for $\gamma = 0$. Thus, in what follows, we always assume the following condition

$$(C_0) \quad 0 < \alpha \leq 1, \quad \beta > (\alpha + 1)\eta \text{ or } \alpha > 1, \quad (\alpha + 1)\eta < \beta < \frac{\alpha}{\alpha - 1}(\alpha + 1)\eta$$

holds. When $0 < \gamma \leq \gamma_*$, from (2.10), we have

$$Det(A) = \frac{\beta u_*(1 - u_*)}{(\gamma + v_*)^2} G(\gamma, u_*),$$

where

$$G(\gamma, u_*) = \gamma(1 - 2u_*) + (1 - u_*)^2. \tag{2.11}$$

Since $0 < u_* < 1$, the sign of $Det(A)$ is the same to the sign of $G(\gamma, u_*)$. So let's investigate the sign of $G(\gamma, u_*)$.

When $\beta > (\alpha + 1)\eta$, it follows from (2.6), (2.7) and (2.11) that for $u_* = u_*^+$,

$$\begin{aligned} G(\gamma, u_*^+) &= -\frac{\eta + \sqrt{Q}}{\beta - \alpha\eta}\gamma + \frac{(\beta - (\alpha + 1)\eta - \sqrt{Q})^2}{4(\beta - \alpha\eta)^2} \\ &= \frac{1}{4(\beta - \alpha\eta)^2} \left(4\gamma(\beta - \alpha\eta)(-\eta - \sqrt{Q}) + (\beta - (\alpha + 1)\eta - \sqrt{Q})^2 \right) \\ &= \frac{1}{4(\beta - \alpha\eta)^2} \left(Q - 4\gamma\sqrt{Q}(\beta - \alpha\eta) - 2\sqrt{Q}(\beta - (\alpha + 1)\eta) + Q \right) \\ &= \frac{\sqrt{Q}}{2(\beta - \alpha\eta)^2} \left(-2\gamma(\beta - \alpha\eta) - \beta + (\alpha + 1)\eta + \sqrt{Q} \right) \\ &< \frac{\sqrt{Q}}{2(\beta - \alpha\eta)^2} \left(-2\gamma(\beta - \alpha\eta) - \beta + (\alpha + 1)\eta + \beta - (\alpha + 1)\eta \right) < 0, \end{aligned} \tag{2.12}$$

where we have used that $\sqrt{Q} = \sqrt{(\beta - (\alpha + 1)\eta)^2 - 4\gamma\eta(\beta - \alpha\eta)} < \beta - (\alpha + 1)\eta$. It follows from (2.12) that (2.9) has one positive root and one negative root. Thus, $E_*^+(u_*^+, v_*^+)$ is a saddle. This result has also been proved in^[35] by graphical approach.

For $u_* = u_*^-$ and $u_* = u_*^{(1)}$, using the similar way, we have

$$G(\gamma, u_*) \begin{cases} > 0, & u_* = u_*^-, \\ = 0, & u_* = u_*^{(1)}. \end{cases} \tag{2.13}$$

To determine the stability of the positive equilibrium $E_*^-(u_*^-, v_*^-)$ of system (2.2), we still need to determine the sign of $Tr(A)$. For $E_*^-(u_*^-, v_*^-)$, it follows from (2.10) that

$$\begin{aligned} Tr(A) &= -u_*^- + \frac{\alpha u_*^- v_*^-}{(1 + \alpha u_*^-)^2} + \frac{\gamma \beta u_*^- v_*^-}{(1 + \alpha u_*^-)(\gamma + v_*^-)^2} \\ &= \frac{u_*^-}{1 + \alpha u_*^-} (\alpha - 1 - 2\alpha u_*^-) + \frac{u_*^-}{1 + \alpha u_*^-} \left(1 - \frac{v_*^-}{v_*^- + \gamma} \right) \frac{\beta v_*^-}{v_*^- + \gamma} \\ &= \frac{u_*^-}{1 + \alpha u_*^-} (\alpha - 1 - 2\alpha u_*^-) + \frac{u_*^-}{1 + \alpha u_*^-} \frac{\beta u_*^- - (1 + \alpha u_*^-)\eta}{\beta u_*^-} \frac{(1 + \alpha u_*^-)\eta}{u_*^-} \\ &= \frac{1}{\beta u_*^- (1 + \alpha u_*^-)} \left(\beta (u_*^-)^2 (\alpha - 1 - 2\alpha u_*^-) + \eta (1 + \alpha u_*^-) ((\beta - \alpha\eta)u_*^- - \eta) \right) \\ &= \frac{1}{\beta u_*^- (1 + \alpha u_*^-)} \left(-2\alpha\beta (u_*^-)^3 + ((\alpha - 1)\beta + (\beta - \alpha\eta)\alpha\eta) (u_*^-)^2 \right. \\ &\quad \left. + (\beta - 2\alpha\eta)\eta u_*^- - \eta^2 \right). \end{aligned} \tag{2.14}$$

For fixed the value of α, β and η , u_*^- can be considered as a function of γ , and then let

$$H = H(\gamma) = -2\alpha\beta (u_*^-)^3 + ((\alpha - 1)\beta + (\beta - \alpha\eta)\alpha\eta) (u_*^-)^2 + (\beta - 2\alpha\eta)\eta u_*^- - \eta^2. \tag{2.15}$$

The sign of $Tr(A)$ is the same to the sign of H . So let's investigate the sign of H .

Under the condition (C_0) , we have $H(0) < 0$. From (2.15), we have

$$H'(\gamma) = (-6\alpha\beta(u_*^-)^2 + 2((\alpha - 1)\beta + (\beta - \alpha\eta)\alpha\eta)u_*^- + (\beta - 2\alpha\eta)\eta) \frac{du_*^-}{d\gamma}.$$

From (2.6), we have

$$\frac{du_*^-}{d\gamma} = -\frac{1}{2(\beta - \alpha\eta)} \frac{1}{2\sqrt{Q}} (-4\eta(\beta - \alpha\eta)) = \frac{\eta}{\sqrt{Q}} > 0, \tag{2.16}$$

which implies that the sign of $H'(\gamma)$ is determined by that of H_1 , where

$$H_1 = H_1(\gamma) = -6\alpha\beta(u_*^-)^2 + 2((\alpha - 1)\beta + (\beta - \alpha\eta)\alpha\eta)u_*^- + (\beta - 2\alpha\eta)\eta. \tag{2.17}$$

In what follows, we investigate the sign of H_1 according to two cases: $\beta \geq 2\alpha\eta$, $\beta < 2\alpha\eta$.

Case I. For $\beta \geq 2\alpha\eta$, let

$$h_1(z) = -6\alpha\beta z^2 + 2((\alpha - 1)\beta + (\beta - \alpha\eta)\alpha\eta)z + (\beta - 2\alpha\eta)\eta. \tag{2.18}$$

Then it is easy to verify that $h_1(z) = 0$ has a unique positive root

$$z_1^* \triangleq \frac{2((\alpha - 1)\beta + (\beta - \alpha\eta)\alpha\eta) + \sqrt{\tilde{Q}}}{12\alpha\beta}, \tag{2.19}$$

where

$$\tilde{Q} = 4((\alpha - 1)\beta + (\beta - \alpha\eta)\alpha\eta)^2 + 24\alpha\beta\eta(\beta - 2\alpha\eta) > 0, \tag{2.20}$$

and we can obtain $h_1(z) > 0$ for $0 < z < z_1^*$ and $h_1(z) < 0$ for $z > z_1^*$.

By $h_1(z) = 0$, it is easy to conclude that $0 < z_1^* < 1$ provided that $h_1(1) < 0$ and $z_1^* \geq 1$ provided that $h_1(1) \geq 0$, where

$$h_1(1) = (\eta - 2)(2\alpha + 1)\beta - 2\alpha\eta^2(\alpha + 1). \tag{2.21}$$

From (2.19) and let $u_*^- = z_1^*$, we can calculate

$$\gamma_c = \frac{(\beta - (\alpha + 1)\eta)^2 - (\beta - \alpha\eta + \eta - 2(\beta - \alpha\eta)z_1^*)^2}{4\eta(\beta - \alpha\eta)}, \tag{2.22}$$

which, together with (2.5), implies that $\gamma_c \leq \gamma_*$ and $\gamma_c = \gamma_*$ if and only if $z_1^* = \frac{\beta - \alpha\eta + \eta}{2(\beta - \alpha\eta)}$.

From (2.16), u_*^- is an increasing function of γ . Therefore, we can conclude that $H_1(\gamma) > 0$ for $\gamma < \gamma_c$, and $H_1(\gamma) < 0$ for $\gamma > \gamma_c$, and $H_1(\gamma) = 0$ for $\gamma = \gamma_c$. So, $H(\gamma)$ has a maximum at $\gamma = \gamma_c$.

Theorem 2.6. *Assumed that $\eta > 0$, either $0 < \alpha \leq 1$ and $\beta > (\alpha + 1)\eta$, or $1 < \alpha < 3$ and $2\alpha\eta \leq \beta < \frac{\alpha}{\alpha - 1}(\alpha + 1)\eta$ are hold. γ_* , γ_c and $H(\gamma)$ are defined by (2.5), (2.22) and (2.15), respectively. Then for fixed $\alpha > 0$, we have the following results on the stability of the positive equilibrium $E_*^-(u_*^-, v_*^-)$.*

(I) For $(\eta - 2)(2\alpha + 1)\beta - 2\alpha\eta^2(\alpha + 1) \geq 0$,

(i) when $H(\gamma_*) \leq 0$, the positive equilibrium $E_*^-(u_*^-, v_*^-)$ of (2.2) is always asymptotically stable for any $0 < \gamma < \gamma_*$;

(ii) when $H(\gamma_*) > 0$, there exists a $\gamma_H^* \in (0, \gamma_*)$, such that the positive equilibrium $E_*^-(u_*^-, v_*^-)$ of (2.2) is asymptotically stable for any $0 < \gamma < \gamma_H^*$ and unstable for $\gamma_H^* < \gamma < \gamma_*$, and system (2.2) undergoes Hopf bifurcation near $E_*^-(u_*^-, v_*^-)$ at $\gamma = \gamma_H^*$;

(II) for $(\eta - 2)(2\alpha + 1)\beta - 2\alpha\eta^2(\alpha + 1) < 0$,

(i) when $H(\gamma_c) < 0$, the positive equilibrium $E_*^-(u_*^-, v_*^-)$ of (2.2) is always asymptotically stable for any $0 < \gamma < \gamma_*$;

(ii) when $H(\gamma_c) > 0$ and $H(\gamma_*) \geq 0$, there exists a $\gamma_H^* \in (0, \gamma_*)$, such that the positive equilibrium $E_*^-(u_*^-, v_*^-)$ of (2.2) is asymptotically stable for any $0 < \gamma < \gamma_H^*$ and unstable for $\gamma_H^* < \gamma < \gamma_*$, and system (2.2) undergoes Hopf bifurcation near $E_*^-(u_*^-, v_*^-)$ at $\gamma = \gamma_H^*$;

(iii) when $H(\gamma_c) > 0$ and $H(\gamma_*) < 0$, there exists $\gamma_H^{(j)} \in (0, \gamma_*)$, $j = 1, 2$, such that the positive equilibrium $E_*^-(u_*^-, v_*^-)$ of (2.2) is asymptotically stable for either $0 < \gamma < \gamma_H^{(1)}$ or $\gamma_H^{(2)} < \gamma < \gamma_*$, and unstable for $\gamma_H^{(1)} < \gamma < \gamma_H^{(2)}$, and system (2.2) undergoes Hopf bifurcation near $E_*^-(u_*^-, v_*^-)$ at $\gamma = \gamma_H^{(j)}$, $j = 1, 2$.

Proof. As can be seen from the above analysis, when the hypothesis is true, and $(\eta - 2)(2\alpha + 1)\beta - 2\alpha\eta^2(\alpha + 1) \geq 0$. From (2.21) and (2.18), we can obtain that $z_1^* \geq 1$ and $h_1(z) > 0$ for any $0 < z < 1$, which, together with (2.17), we have $H_1(\gamma) > 0$ for any $0 < \gamma < \gamma_*$.

Thus, it follows from (2.15)-(2.17) that $H(\gamma)$ is a strictly increasing function of γ ($0 < \gamma < \gamma_*$). And because of $H(0) < 0$, it is easy to obtain that when $H(\gamma_*) \leq 0$, $H(\gamma) < 0$ for any $0 < \gamma < \gamma_*$, by (2.14), $Tr(A) < 0$ and the positive equilibrium $E_*^-(u_*^-, v_*^-)$ of (2.2) is always asymptotically stable for any $0 < \gamma < \gamma_*$. While for $H(\gamma_*) > 0$, there must exist a $\gamma_H^* \in (0, \gamma_*)$, such that the positive equilibrium $E_*^-(u_*^-, v_*^-)$ of (2.2) is asymptotically stable for any $0 < \gamma < \gamma_H^*$ and unstable for $\gamma_H^* < \gamma < \gamma_*$.

Next, in order to confirm the existence of the Hopf bifurcation, we need to check the transversal condition. Taking the derivation of both sides of (2.9) with respect to γ , and when $\gamma = \gamma_H^*$, we have

$$\left(\frac{dRe(\lambda)}{d\gamma}\right)_{\gamma=\gamma_H^*} = \frac{1}{2} \left(\frac{dTr(A)}{d\gamma}\right)_{\gamma=\gamma_H^*} = \frac{H_1}{2\beta u_*^-(1 + \alpha u_*^-)} \frac{du_*^-}{d\gamma},$$

by the analysis above, we have $H_1 > 0$ for $\gamma = \gamma_H^*$. Then it is easy to see that

$$\left(\frac{dTr(A)}{d\gamma}\right)_{\gamma=\gamma_H^*} > 0.$$

Therefore, the transversal condition of the Hopf bifurcation is satisfied. And we can obtain that system (2.2) undergoes Hopf bifurcation near $E_*^-(u_*^-, v_*^-)$ at $\gamma = \gamma_H^*$.

Using the similar way as above, if $(\eta - 2)(2\alpha + 1)\beta - 2\alpha\eta^2(\alpha + 1) < 0$, we can obtain that $0 < z_1^* < 1$, and $h_1(z) > 0$ for any $0 < z < z_1^*$ and $h_1(z) < 0$ for any $0 < z < 1$. This, together with (2.22) and (2.15)-(2.17), implies that $H(\gamma)$ has a maximum at $0 < \gamma = \gamma_c < \gamma_*$. Thus, it is easy to verify that the conclusion of (II) holds.

In this way, the proof of the theorem is complete. □

Remark 2.7. The conclusion in Theorem 2.6 (II)(iii) has also shown that the Allee effect of the predator can induce the stability switches for the positive equilibrium $E_*^-(u_*^-, v_*^-)$, i.e., the stability of the positive equilibrium $E_*^-(u_*^-, v_*^-)$ can change from stability to instability and back to stability with the increasing of strength of the Allee effect of the predator.

Case II. For $\beta < 2\alpha\eta$, we only need to consider the situation $\alpha > 1$ of the condition C_0 under the the case for $\beta < 2\alpha\eta$. From (2.18), we find that the axis of symmetry of $h(z)$ must be on the right and the number of positive roots of $h_1(z) = 0$ needs further discussion for the sign of \tilde{Q} . It follows from (2.20) that

$$\begin{aligned} \tilde{Q} &= 4((\alpha - 1)\beta + (\beta - \alpha\eta)\alpha\eta)^2 + 24\alpha\beta\eta(\beta - 2\alpha\eta) \\ &= (4(\alpha - 1)(\alpha - 1 + 8\alpha\eta) + 4\alpha\eta(\alpha\eta + 6))\beta^2 - 8\alpha^2\eta^2(\alpha + 5 + \alpha\eta)\beta + 4\alpha^4\eta^4, \end{aligned}$$

and the discriminant of \tilde{Q} is

$$\begin{aligned} &(8\alpha^2\eta^2(\alpha + 5 + \alpha\eta))^2 - 16\alpha^4\eta^4(4(\alpha - 1)(\alpha - 1 + 8\alpha\eta) + 4\alpha\eta(\alpha\eta + 6)) \\ &= 384\alpha^4\eta^4(2\alpha + \alpha\eta + 4) \triangleq \hat{Q} > 0. \end{aligned}$$

Thus, $\tilde{Q} = 0$ always have two positive roots β_1 and β_2 , where

$$\beta_{1,2} = \frac{\alpha^2\eta^2(\alpha + 5 + \alpha\eta) \mp \alpha^2\eta^2\sqrt{12\alpha + 6\alpha\eta + 24}}{(\alpha - 1 + \alpha\eta)^2 + 6\alpha\eta}. \tag{2.23}$$

It is easy to conclude that $\tilde{Q} > 0$ for either $0 < \beta < \beta_1$ or $\beta > \beta_2$, and $\tilde{Q} \leq 0$ for $\beta_1 \leq \beta \leq \beta_2$. Then it is easy to verify that $h_1(z) = 0$ has two positive roots

$$z_{1,2}^* = \frac{2((\alpha - 1)\beta + (\beta - \alpha\eta)\alpha\eta) \pm \sqrt{\tilde{Q}}}{12\alpha\beta} \tag{2.24}$$

for $\tilde{Q} > 0$. And we can obtain that $h_1(z) < 0$ for either $0 < z < z_2^*$ or $z > z_1^*$, and $h_1(z) > 0$ for $z_2^* < z < z_1^*$.

Next, using the similar method as Case I, we need to investigate the value between $z_{1,2}^*$ and 1 in the following two cases.

- (i) When $h_1(1) > 0$, it is easy to obtain that $0 < z_2^* < 1 < z_1^*$.
- (ii) When $h_1(1) \leq 0$, we need to judge the sign of $\bar{z} - 1$, where \bar{z} is the the axis of symmetry of $h_1(z)$ and $\bar{z} = \frac{(\alpha-1)\beta+(\beta-\alpha\eta)\alpha\eta}{6\alpha\beta}$. It is obvious that $0 < z_2^* < z_1^* < 1$ for $\bar{z} < 1$ and $1 \leq z_2^* < z_1^*$ for $\bar{z} \geq 1$.

From (2.24), let $u_*^- = z_1^*$ and $u_*^- = z_2^*$, respectively, we can calculate

$$\gamma_c = \frac{(\beta - (\alpha + 1)\eta)^2 - (\beta - \alpha\eta + \eta - 2(\beta - \alpha\eta)z_1^*)^2}{4\eta(\beta - \alpha\eta)}$$

and

$$\gamma_{2c} = \frac{(\beta - (\alpha + 1)\eta)^2 - (\beta - \alpha\eta + \eta - 2(\beta - \alpha\eta)z_2^*)^2}{4\eta(\beta - \alpha\eta)}. \tag{2.25}$$

Therefore, When $h_1(1) > 0$, we have $H_1 < 0$ for $0 < \gamma < \gamma_{2c}$ and $H_1 > 0$ for $\gamma_{2c} < \gamma < \gamma_*$, so $H(\gamma)$ has a minimum at $\gamma = \gamma_{2c}$ for $0 < \gamma < \gamma_*$. When $h_1(1) \leq 0$ and $\bar{z} \geq 1$, we can conclude that $H_1 < 0$ for $0 < \gamma < \gamma_*$.

When $h_1(1) \leq 0$ and $\bar{z} < 1$, we can conclude that $H_1 > 0$ for $\gamma_{2c} < \gamma < \gamma_c$ and $H_1 < 0$ for either $0 < \gamma < \gamma_{2c}$ or $\gamma_c < \gamma < \gamma_*$. So $H(\gamma)$ has a minimum at $\gamma = \gamma_{2c}$ and a maximum at $\gamma = \gamma_c$ for $0 < \gamma < \gamma_*$.

Theorem 2.8. Assumed that $\eta > 0$, either $1 < \alpha < 3$ and $(\alpha + 1)\eta < \beta < 2\alpha\eta$, or $\alpha \geq 3$ and $(\alpha + 1)\eta < \beta < \frac{\alpha}{\alpha-1}(\alpha + 1)\eta$ are hold. γ_* , γ_c , $H(\gamma)$ and $\beta_{1,2}$ are defined by (2.5), (2.22), (2.15) and (2.23), respectively. Then for fixed α , we have the following results on the stability of the positive equilibrium $E_*^-(u_*^-, v_*^-)$.

- (I) When $\beta_1 \leq \beta \leq \beta_2$, the positive equilibrium $E_*^-(u_*^-, v_*^-)$ of (2.2) is always asymptotically stable for any $0 < \gamma < \gamma_*$;
- (II) when $0 < \beta < \beta_1$ or $\beta > \beta_2$,
 - (i) and $(\eta - 2)(2\alpha + 1)\beta - 2\alpha\eta^2(\alpha + 1) > 0$, we have the same results as in Theorem 2.6 (I);
 - (ii) $(\eta - 2)(2\alpha + 1)\beta - 2\alpha\eta^2(\alpha + 1) \leq 0$, and $\bar{z} \geq 1$, the positive equilibrium $E_*^-(u_*^-, v_*^-)$ of (2.2) is always asymptotically stable for any $0 < \gamma < \gamma_*$, where $\bar{z} = \frac{(\alpha - 1)\beta + (\beta - \alpha\eta)\alpha\eta}{6\alpha\beta}$;
 - (iii) $(\eta - 2)(2\alpha + 1)\beta - 2\alpha\eta^2(\alpha + 1) \leq 0$, and $\bar{z} < 1$, we have the same results as in Theorem 2.6 (II).

Proof. When $\beta_1 \leq \beta \leq \beta_2$, it follows from (2.18) and (2.23) that we have $\tilde{Q} \leq 0$ and $h_1(z) < 0$ for any $0 < z < 1$. By (2.17) we have $H_1(\gamma) < 0$ for any $0 < \gamma < \gamma_*$, and in combination with the condition $H(0) < 0$, we can obtain that $H(\gamma) < 0$ for any $0 < \gamma < \gamma_*$. Then the positive equilibrium $E_*^-(u_*^-, v_*^-)$ of (2.2) is always asymptotically stable for any $0 < \gamma < \gamma_*$.

When $0 < \beta < \beta_1$ or $\beta > \beta_2$, it follows from (2.18) and (2.23) that we have $\tilde{Q} > 0$. Thus, $h_1(z)$ has two positive roots $z_{1,2}^*$ and $h_1(z) > 0$ for $z_2^* < z < z_1^*$, and $h(z) < 0$ for either $0 < z < z_2^*$ or $z > z_1^*$. Then using the same way as the proof of Theorem 2.6.

(i) when $(\eta - 2)(2\alpha + 1)\beta - 2\alpha\eta^2(\alpha + 1) > 0$, we have $0 < z_2^* < 1 < z_1^*$, it follows from (2.15)–(2.18) that $H(\gamma)$ has a minimum at $\gamma = \gamma_{2c}$ for $0 < \gamma < \gamma_*$.

Since $H(0) < 0$, we need to judge the sign of $H(\gamma_*)$. It is easy to find that we can obtain the same conclusion as Theorem 2.6 (I).

(ii) When $(\eta - 2)(2\alpha + 1)\beta - 2\alpha\eta^2(\alpha + 1) \leq 0$ and $\bar{z} \geq 1$, it is easy to obtain that $h_1(z) < 0$ for any $0 < z < 1$. It follows from (2.15)–(2.18) that $H(\gamma)$ is strictly decreasing for any $0 < \gamma < \gamma_*$. And in combination with the condition $H(0) < 0$, the positive equilibrium $E_*^-(u_*^-, v_*^-)$ of (2.2) is always asymptotically stable for any $0 < \gamma < \gamma_*$.

(iii) When $(\eta - 2)(2\alpha + 1)\beta - 2\alpha\eta^2(\alpha + 1) \leq 0$ and $\bar{z} < 1$, it is easy to obtain that $h_1(z) < 0$ for either $0 < z < z_2^*$ or $z_1^* < z < 1$, and $h_1(z) > 0$ for $z_2^* < z < z_1^*$. Then from (2.15)–(2.18), $H(\gamma)$ has a minimum at $\gamma = \gamma_{2c}$ and a maximum at $\gamma = \gamma_c$ for $0 < \gamma < \gamma_*$. Thus, we can use the same way as the proof of Theorem 2.6 (II) to obtain the conclusion of this Theorem. \square

2.2 Numerical Simulations for the Stability and Periodic Solutions

Now, we numerically show the theoretical results in the rest of this subsection. For $\alpha = 0.5$, define the curves f_j , $j = 1, 2, 3, 4$ in the $\eta - \beta$ plane by

$$\begin{aligned} f_1 : \beta &= 1.5\eta, & f_2 : (\eta - 2)(2\alpha + 1)\beta - 2\alpha\eta^2(\alpha + 1) &= 0, \\ f_3 : H(\gamma_c) &= 0, & f_4 : H(\gamma_*) &= 0. \end{aligned}$$

These four curves f_j , $j = 1, 2, 3, 4$ are plotted in Figure 2.1. Denote the regions in Figure 2.1 by R_j , $j = 0, 1, 2$.

When (η, β) lies in the region R_0 , the positive equilibrium E_*^- is always asymptotically stable for any $0 < \gamma < \gamma_*$. When (η, β) lies in the region R_1 , there exists a Hopf bifurcation value γ_H^* , such that the positive equilibrium E_*^- is asymptotically stable for $0 < \gamma < \gamma_H^*$ and unstable for $\gamma_H^* < \gamma < \gamma_*$.

For numerical simulations, taking $(\eta, \beta) = (2.5, 7)$ as marked by $P_1 \in R_1$ in Figure 2.1, we have $(\eta - 2)(2\alpha + 1)\beta - 2\alpha\eta^2(\alpha + 1) \approx -2.375 < 0$. It follows from (2.5) that $\gamma_* \approx 0.1876$, from (2.19), we have $z_1^* \approx 0.9283$, and then by (2.22), we have $\gamma_c \approx 0.0814$. Furthermore, from

(2.15), we have $H(\gamma_c) \approx 1.7714 > 0$ and $H(\gamma_*) \approx 1.1340 > 0$. Therefore, the condition $II(ii)$ of Theorem 2.6 is satisfied for $\alpha = 0.5$, $\beta = 7$, $\eta = 2.5$. From $H(\gamma) = 0$, we have

$$\gamma_H^* \approx 0.1286.$$

It follows from Theorem 2.6 that for $\alpha = 0.5$, $\beta = 7$, $\eta = 2.5$, E_*^- is asymptotically stable for $0 < \gamma < \gamma_H^* \approx 0.1286$, as shown in Figure 2.2 (a) for $\gamma = 0.1$, and unstable for $\gamma_H^* < \gamma < \gamma_*$. The black and red points in Figure 2.2 (a) are the positive equilibria $E_*^-(0.5266, 0.5980)$ and $E_*^+(0.9082, 0.1336)$, respectively.

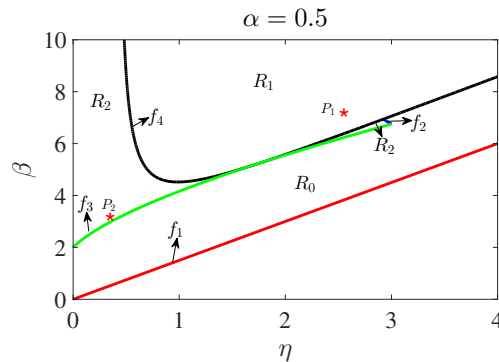


Figure 2.1. Bifurcation diagram for the positive equilibrium $E_*^-(u_*^-, v_*^-)$ of system (2.2) in the $\eta - \beta$ plane for $\alpha = 0.5$.

For $\gamma_H^* < \gamma < \gamma_*$, E_*^- is unstable and the system undergoes Hopf bifurcation at $\gamma = \gamma_H^*$. Taking $\gamma = 0.125 < \gamma_H^*$, the numerical simulation shows that there exists an unstable periodic orbit which is inner stable (with the stable equilibrium E_*^-) and out unstable, as shown in Figure 2.2 (b) with different initial values (0.5576, 0.77875) and (0.5576, 0.7775). The black and red points in Figure 2.2 (b) are $E_*^-(0.5576, 0.7775)$ by black point and $E_*^+(0.8771, 0.1767)$. This numerical simulation also implies that Hopf bifurcation at $\gamma = \gamma_H^*$ is subcritical.

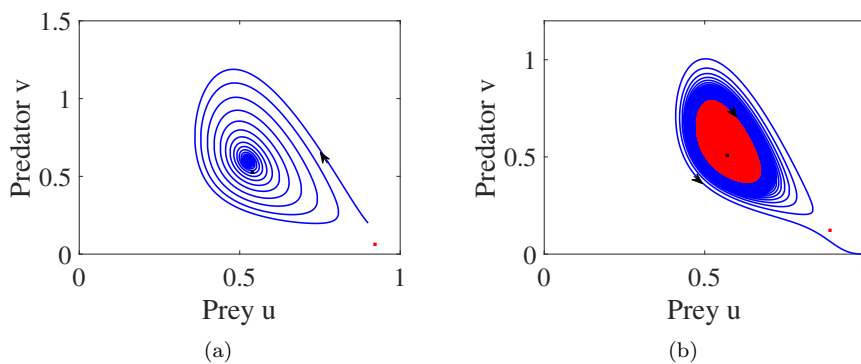


Figure 2.2. The phase portrait of system (2.2) for $(\eta, \beta) \in R_1$ for $\alpha = 0.5$, $\eta = 2.5$ and $\beta = 7$ with the increasing of γ . (a): $\gamma = 0.1$; (b): $\gamma = 0.125$.

When (η, β) lies in the region R_2 , there exists two Hopf bifurcation values $\gamma_H^{(1)}$ and $\gamma_H^{(2)}$, such that the positive equilibrium E_*^- is asymptotically stable for either $0 < \gamma < \gamma_H^{(1)}$ or $\gamma_H^{(2)} < \gamma < \gamma_*$ and unstable for $\gamma_H^{(1)} < \gamma < \gamma_H^{(2)}$.

For numerical simulations, taking $(\eta, \beta) = (0.3, 3)$ as marked by $P_2 \in R_2$ in Figure 2.1. Similarly, we can calculate $(\eta - 2)(2\alpha + 1)\beta - 2\alpha\eta^2(\alpha + 1) \approx -10.3350 < 0$, $\gamma_* \approx 1.9013$ and $\gamma_c \approx 0.7442$. Furthermore, from (2.15), we have $H(\gamma_c) \approx 0.0051 > 0$ and $H(\gamma_*) \approx -0.4762 < 0$. Therefore, the condition II (iii) of Theorem 2.6 is satisfied for $\alpha = 0.5$, $\beta = 3$, and $\eta = 0.3$. From $H(\gamma) = 0$, we have

$$\gamma_H^{(1)} \approx 0.4414, \quad \gamma_H^{(2)} \approx 1.001.$$

It follows from Theorem 2.6 that for $\alpha = 0.5$, $\beta = 3$, and $\eta = 0.3$, E_*^- is asymptotically stable for either $0 < \gamma < \gamma_H^{(1)}$ or $\gamma_H^{(2)} < \gamma < 1.9013$, as shown in Figure 2.3 (a) for $\gamma = 0.4 < \gamma_H^{(1)}$ and in Figure 2.3 (d) for $\gamma = 1.1 > \gamma_H^{(2)}$.

For $\gamma_H^{(1)} < \gamma < \gamma_H^{(2)}$, E_*^- is unstable and the system undergoes Hopf bifurcations at $\gamma = \gamma_H^{(1)}$ and $\gamma = \gamma_H^{(2)}$. For $\gamma = 0.5 > \gamma_H^{(1)}$ and close to $\gamma_H^{(1)}$, Figure 2.3 (b) shows the existence of the stable periodic orbit with different initial values $(0.1686, 1.25)$ and $(0.9367, 0.1)$. For $\gamma = 0.98 > \gamma_H^{(2)}$ and close to $\gamma_H^{(2)}$, Figure 2.3 (c) shows the existence of the stable periodic orbit with different initial values $(0.2412, 0.87)$ and $(0.8640, 0.3)$. The numerical simulations in Figs.2.3 (b) and 2.3 (c) also show that the Hopf bifurcations at $\gamma = \gamma_H^{(1)}$ and $\gamma = \gamma_H^{(2)}$ are both supercritical.

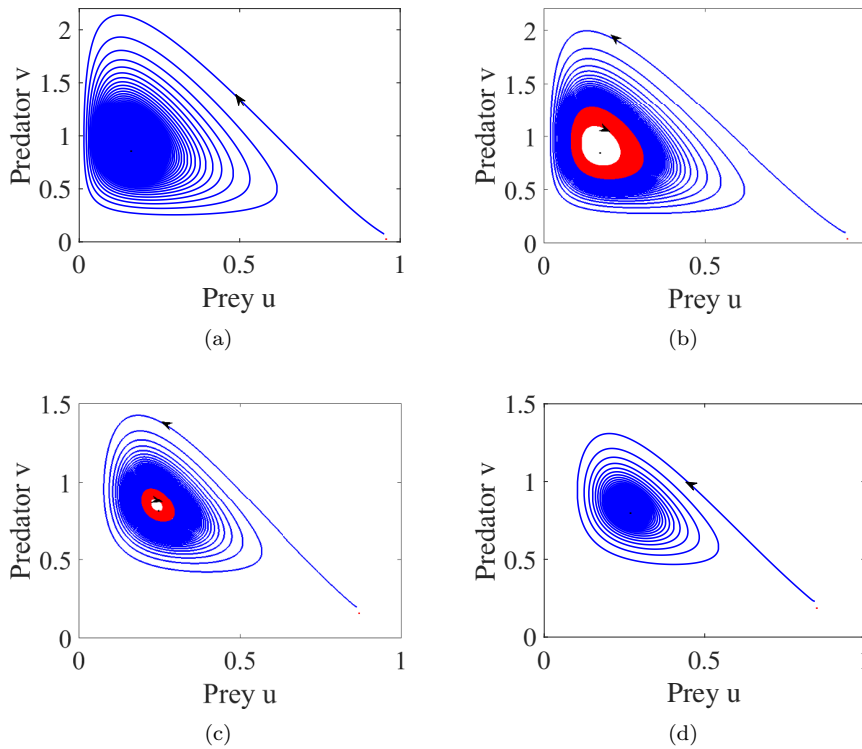


Figure 2.3. The phase portrait of system (2.2) for $(\eta, \beta) \in R_2$ for $\alpha = 0.5$, $\eta = 0.3$ and $\beta = 3$ with the increasing of γ . (a): $\gamma = 0.4$; (b): $\gamma = 0.5$; (c): $\gamma = 0.98$; (d): $\gamma = 1.1$.

Hopf bifurcations at $\gamma = \gamma_H^{(1)}$ and $\gamma = \gamma_H^{(2)}$ only show that there exist periodic orbits near the neighborhood of bifurcation values, but we can not prove whether there exist periodic orbits for any given $\gamma \in (\gamma_H^{(1)}, \gamma_H^{(2)})$ or not. Taking a series of values of γ close to $\gamma_H^{(1)}$ in order

from small to large, Figure 2.4 (a) shows that the amplitude of periodic orbit increases as γ is increased. Where $g_i (i = 1, 2, 3)$ represent the periodic orbits for different values of $\gamma_i (i = 1, 2, 3)$, respectively, and $\gamma_1 = 0.48, \gamma_2 = 0.5, \gamma_3 = 0.58$.

Similarly, taking a series of values of γ close to $\gamma_H^{(2)}$ in order from small to large, Figure 2.4 (b) shows that the amplitude of periodic orbit decreases as γ is increased. Where $g_i (i = 4, 5, 6)$ represent the periodic orbits for different values of $\gamma_i (i = 1, 2, 3)$, respectively, and $\gamma_4 = 0.78, \gamma_5 = 0.88, \gamma_6 = 0.98$.

Figure 2.4 also shows that the stable periodic orbit exists for values of γ far from the values of Hopf bifurcations at $\gamma = \gamma_H^{(1)}$ and $\gamma = \gamma_H^{(2)}$.

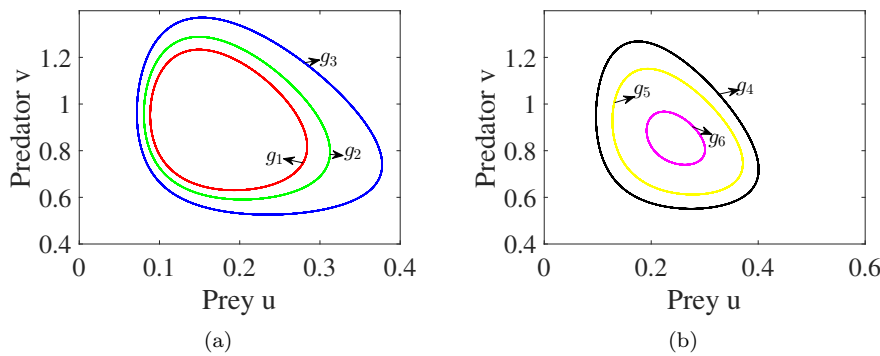


Figure 2.4. The phase portrait of system (2.2) for $(\eta, \beta) \in R_2$ with $\alpha = 0.5, \eta = 0.3$ and $\beta = 3$. (a): $g_i (i = 1, 2, 3)$ represent the periodic orbits of $\gamma_1 = 0.48, \gamma_2 = 0.5$ and $\gamma_3 = 0.58$, respectively. (b): $g_i (i = 4, 5, 6)$ represent the periodic orbits of $\gamma_4 = 0.78, \gamma_5 = 0.88$ and $\gamma_6 = 0.98$, respectively.

3 Diffusion-driven Turing Instability and Spatial Patterns

3.1 Stability and Diffusion-driven Turing Instability

It is easy to verify that system (2.1) has the same constant equilibrium with (2.2). In this subsection, we investigate system (2.1) under the assumption that the positive equilibrium $E_*^-(u_*^-, v_*^-)$ of system (2.2) is asymptotically stable, i.e., for $E_*^-(u_*^-, v_*^-)$, we always assume that $Tr(A) < 0, Det(A) > 0$.

To study the stability of the positive equilibrium $E_*^-(u_*^-, v_*^-)$ of system (2.1), we should consider the roots of the characteristic equation of the linearized system of system (2.1). The linearized system of system (2.1) at $E_*^-(u_*^-, v_*^-)$ is:

$$\begin{pmatrix} \frac{\partial u}{\partial t} \\ \frac{\partial v}{\partial t} \end{pmatrix} = \begin{pmatrix} d_1 \Delta & 0 \\ 0 & d_2 \Delta \end{pmatrix} \begin{pmatrix} u \\ v \end{pmatrix} + A \begin{pmatrix} u \\ v \end{pmatrix}. \tag{3.1}$$

Assume that

$$\begin{pmatrix} u \\ v \end{pmatrix} = \begin{pmatrix} u_*^- \\ v_*^- \end{pmatrix} + \begin{pmatrix} a \\ b \end{pmatrix} \exp(\lambda t + i(\mathbf{k} \cdot \mathbf{r})) \tag{3.2}$$

is the solution of (3.1), where $k = |\mathbf{k}|$ is called the wave number and $\mathbf{k} = (k_x, k_y)$ is the wave number vector, \mathbf{r} represent the two-dimensional spatial vector and $(a, b)^T$ is the constant undetermined column vector.

Substituting (3.2) into (3.1), we have

$$(\lambda I - A_k) \begin{pmatrix} a \\ b \end{pmatrix} = 0$$

where I is a 2×2 unit matrix, $A_k = A - \text{diag}(d_1 k^2, d_2 k^2)$ for $k \geq 0$. Thus, the characteristic equation of (3.1) is

$$\lambda^2 - T_k \lambda + D_k = 0, \tag{3.3}$$

where

$$T_k = \text{Tr}(A) - k^2(d_1 + d_2), \quad D_k = d_1 d_2 k^4 - (d_1 a_{22} + d_2 a_{11})k^2 + \text{Det}(A). \tag{3.4}$$

Obviously, $T_k < 0$ for any $k \geq 0$ and $\gamma \geq 0$ when $\text{Tr}(A) < 0$. In particular, when $\gamma = 0$, it follows from (2.10) that $a_{22} = 0$. And then by the basic assumption $\text{Tr}(A) < 0$ and $\text{Det}(A) > 0$ in this subsection that $a_{11} < 0$ and

$$D_k = d_1 d_2 k^4 - (d_1 a_{22} + d_2 a_{11})k^2 + \text{Det}(A) > 0.$$

Therefore, under the basic assumption $\text{Tr}(A) < 0$ and $\text{Det}(A) > 0$ in this subsection, when $\gamma = 0$, the positive equilibrium of $E_*^-(u_*^-, u_*^-)$ is always asymptotically stable for any $d_1, d_2 \geq 0$. That is to say that there is no diffusion-driven Turing instability for system (2.1) without Allee effect ($\gamma = 0$).

In the following, we investigate whether diffusion-driven Turing instability for system (2.1) with $0 < \gamma < \gamma_*$ can occur or not. For this purpose, we need to judge the sign of D_k . Firstly, when $0 < d_1 \leq d_2$, we have

$$-(d_1 a_{22} + d_2 a_{11}) \geq -(d_2 a_{11} + d_2 a_{22}) = -d_2(a_{11} + a_{22}) > 0,$$

which implies that $D_k > 0$ for any $k \geq 0$. So, the diffusion of system (2.1) does not influence the stability of the positive equilibrium of $E_*^-(u_*^-, u_*^-)$ when $0 < d_1 \leq d_2$.

In what follows, we always assume that $d_1 > d_2$. It is well-known that Turing instability occurs only when the following two conditions

$$(C_1) \quad d_1 a_{22} + d_2 a_{11} > 0$$

and

$$(C_2) \quad 4d_1 d_2 \text{Det}(A) - (d_1 a_{22} + d_2 a_{11})^2 < 0$$

are satisfied. When (C₁) and (C₂) hold, there exist at least one positive number k such that $D_k < 0$, which implies that $E_*^-(u_*^-, u_*^-)$ is unstable. This instability is induced by the diffusion and also called diffusion-driven Turing instability.

In the following, we choose d_1 as a parameter to investigate the stability and diffusion-driven Turing instability and we have the following results.

Theorem 3.1. *For the positive equilibrium $E_*^-(u_*^-, v_*^-)$, assume that $\alpha, \eta > 0$, $\beta > (\alpha + 1)\eta$, $0 < \gamma < \gamma_*$, $\text{Tr}(A) < 0$, and $\text{Det}(A) > 0$. Define*

$$d_{1T}^* = \frac{-2d_2(a_{11}a_{22} - 2\text{Det}(A)) + \sqrt{Q_1}}{2a_{22}^2}, \tag{3.5}$$

where

$$Q_1 = -16d_2^2 a_{11} a_{22} \text{Det}(A) + 16d_2^2 (\text{Det}(A))^2.$$

- (i) When $0 < d_1 < d_{1T}^*$, the positive equilibrium $E_*^-(u_*^-, v_*^-)$ of (2.1) is asymptotically stable.
- (ii) When $d_1 > d_{1T}^*$, the positive equilibrium $E_*^-(u_*^-, v_*^-)$ of (2.1) is unstable, and system (2.1) undergoes Turing bifurcation at $d_1 = d_{1T}^{(2)}$.

Proof. Firstly, we notice that for the case without diffusion, the positive equilibrium E_*^- is stable under the assumption. Keep in mind that $T_k < 0$ for any $k \geq 0$ when $\text{Tr}(A) < 0$ in what follows.

By (2.10), $a_{22} > 0$ for $0 < \gamma < \gamma_*$. This, together with $\text{Tr}(A) = a_{11} + a_{22} < 0$, implies that $a_{11} < 0$. It is easy to verify that the condition (C₁) holds when $d_1 > -\frac{a_{11}}{a_{22}}d_2 \triangleq d_1^*$, where

$$d_1^* \triangleq -\frac{a_{11}}{a_{22}}d_2 > 0.$$

By the expression of (C₂), it is easy to see that (C₂) is equivalent to the following condition

$$g(d_1) = a_{22}^2 d_1^2 + 2d_2(a_{11}a_{22} - 2\text{Det}(A))d_1 + d_2^2 a_{11}^2 > 0. \tag{3.6}$$

Since $a_{11}a_{22} < 0$, we have

$$Q_1 = 4d_2^2(a_{11}a_{22} - 2\text{Det}(A))^2 - 4a_{22}^2 d_2^2 a_{11}^2 = -16d_2^2 a_{11} a_{22} \text{Det}(A) + 16d_2^2 (\text{Det}(A))^2 > 0,$$

which implies that the quadratic equations $g(d_1) = 0$ has two positive roots $d_{1T}^{(1)}$ and $d_{1T}^{(2)}$ with

$$0 < d_{1T}^{(1)} = \frac{-2d_2(a_{11}a_{22} - 2\text{Det}(A)) - \sqrt{Q_1}}{2a_{22}^2} < d_{1T}^{(2)} = \frac{-2d_2(a_{11}a_{22} - 2\text{Det}(A)) + \sqrt{Q_1}}{2a_{22}^2}, \tag{3.7}$$

and $g(d_1) < 0$ for $d_{1T}^{(1)} < d_1 < d_{1T}^{(2)}$, $g(d_1) > 0$ for $0 < d_1 < d_{1T}^{(1)}$ or $d_1 > d_{1T}^{(2)}$. When $d_1 = d_1^*$, we have

$$g(d_1^*) = a_{22}^2 \frac{a_{11}^2}{a_{22}^2} d_2^2 - 2d_2 \frac{a_{11}d_2}{a_{22}} (a_{11}a_{22} - 2\text{Det}(A)) + a_{11}^2 d_2^2 = \frac{4d_2^2 a_{11} \text{Det}(A)}{a_{22}} < 0.$$

So, we have the following inequality

$$0 < d_{1T}^{(1)} < d_1^* < d_{1T}^{(2)}.$$

In addition, it is easy to verify that when $0 \leq d_1 \leq d_1^*$, $d_1 a_{22} + d_2 a_{11} \leq 0$, which, together with $\text{Det}(A) > 0$ and (3.4), implies that $D_k > 0$ for any $k > 0$. When $d_1^* < d_1 < d_{1T}^{(2)}$, $g(d_1) < 0$, which, together with (3.4), also implies that $D_k > 0$ for any $k > 0$. Therefore, for any $0 \leq d_1 < d_{1T}^{(2)}$, $D_k > 0$ for any $k > 0$.

When $d_1 > d_{1T}^{(2)}$, the conditions (C₁) and (C₂) holds and there exists $k_1, k_2 > 0$ such that $D_k < 0$ for $k_1 < k < k_2$. Letting $d_{1T}^* = d_{1T}^{(2)}$ for the simpleness of notations, we complete the proof of Theorem 3.1. □

Remark 3.2. By (3.7) and $\text{Tr}(A) < 0$, $\text{Det}(A) > 0$, $a_{22} > 0$, we have

$$\begin{aligned} d_{1T}^{(2)} - d_2 &= \frac{-2d_2(a_{11}a_{22} - 2\text{Det}(A)) + \sqrt{Q_1} - 2d_2 a_{22}^2}{2a_{22}^2} \\ &= \frac{-2d_2 a_{22}(a_{11} + a_{22}) + 4d_2 \text{Det}(A) + \sqrt{Q_1}}{2a_{22}^2} \\ &> 0, \end{aligned}$$

which implies that $d_{1T}^* = d_{1T}^{(2)} > d_2$.

Remark 3.3. At the Turing bifurcation value $d_1 = d_{1T}^*$. The critical wave number k_T can be determined by

$$k_T = \sqrt[4]{\frac{\text{Det}(A)}{d_1 d_2}},$$

at which $D_{k_T} = 0$.

Remark 3.4. As pointed out by Murray^[25], there are two different interactions in the biological sense that lead to essentially different reactions: predators spread faster than prey, and vice versa. In this paper, when the Allee effect exists in predator, Turing instability occurs for the situation in which the prey spreads faster than the predator. The similar result has been observed for the predator-prey model with hunting cooperation by Capone et al.^[7].

3.2 Numerical Investigation of Spatial Patterns

We numerically show the theoretical results of Theorem 3.1 in this section. If we choose $\alpha = 0.5$, $\beta = 4$, $\eta = 1$, then the positive equilibrium $E_*^-(u_*^-, v_*^-)$ exists for $0 < \gamma < 0.4464$. Taking $d_2 = 0.1$, we can obtain the graph of the d_1 about γ as shown in Figure 3.1, where $L_T : d_1 = d_{1T}^*$ and the shaded area represents the stable region of the positive equilibrium $E_*^-(u_*^-, v_*^-)$. So, the Turing instability will occur when $d_1 > d_{1T}^*$ and $0 < \gamma < 0.4464$.

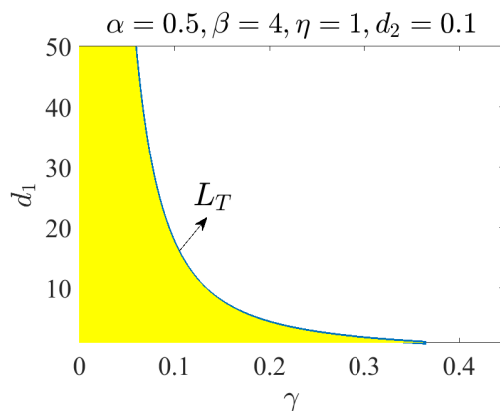


Figure 3.1. Let $\alpha = 0.5$; $\eta = 1$; $d_2 = 0.1$, and $\beta = 4$, the expression of L_T is $d_1 = d_{1T}^*$.

In Figure 3.1, we take a series of numerical simulations in the Turing domain for fixed $\alpha = 0.5$, $\beta = 4$, $\eta = 1$, $d_2 = 0.1$. Let $\gamma = 0.175$ and by calculation we have $d_{1T}^* \approx 5.7147$. The different types of spatial patterns are observed with the various values of the diffusion coefficient d_1 of the prey. And here we show the pattern formation about the prey species u in the following simulations.

Firstly, letting $d_1 = 6$, Figure 3.2 (a)–(f) show the evolution process of the spatial patterns of the u population, we can find that the spot pattern form as Figure 3.2 (f).

Then, letting $d_1 = 7.5$, Figure 3.3 (a)–(f) show the evolution process of the spatial patterns of the u population, we can find that the spot-strip pattern form as Figure 3.3 (f). And the number of spot pattern is more than the strip pattern.

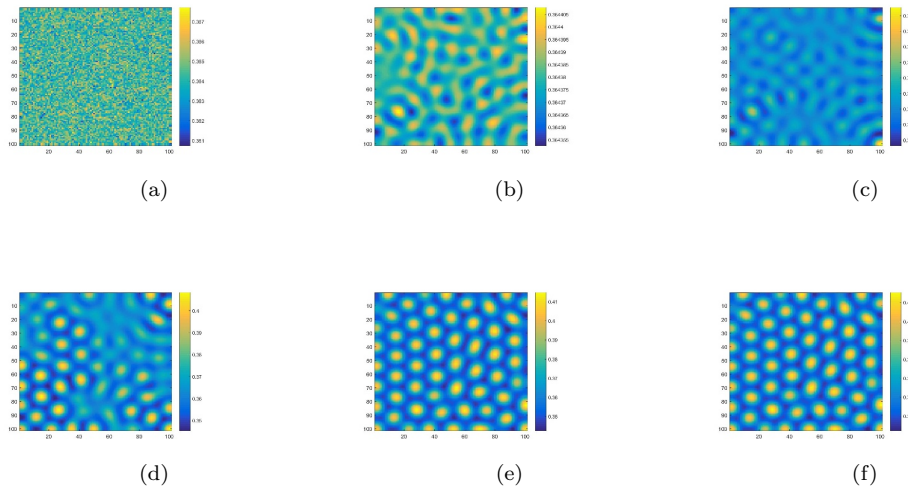


Figure 3.2. Snapshots of contour pictures of the time evolution of the prey population with $\alpha = 0.5, \beta = 4, \eta = 1, d_2 = 0.1, \gamma = 0.175, d_1 = 6$. (a) $t = 0$; (b) $t = 100000$; (c) $t = 3050000$; (d) $t = 3650000$; (e) $t = 4650000$; (f) $t = 5000000$.

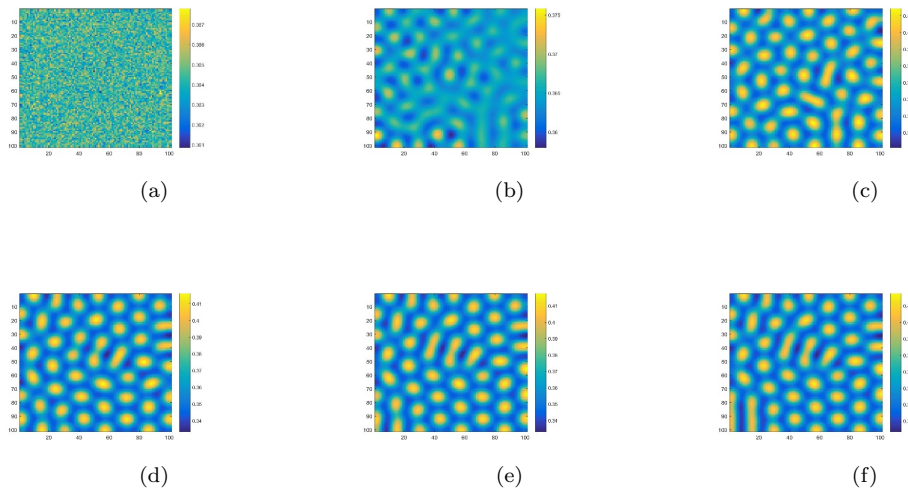


Figure 3.3. Snapshots of contour pictures of the time evolution of the prey population with $\alpha = 0.5, \beta = 4, \eta = 1, d_2 = 0.1, \gamma = 0.175, d_1 = 7.5$. (a) $t = 0$; (b) $t = 550000$; (c) $t = 950000$; (d) $t = 2550000$; (e) $t = 4350000$; (f) $t = 5000000$.

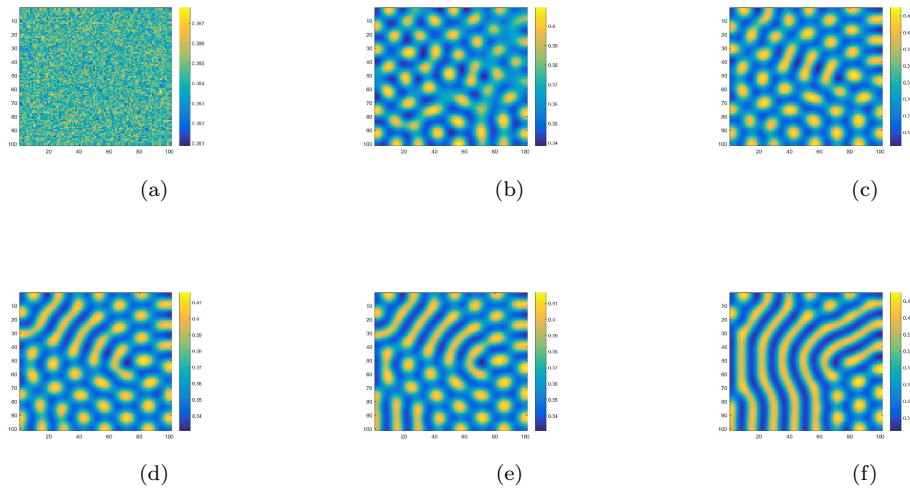


Figure 3.4. Snapshots of contour pictures of the time evolution of the prey population with $\alpha = 0.5$, $\beta = 4$, $\eta = 1$, $d_2 = 0.1$, $\gamma = 0.175$, $d_1 = 8$. (a) $t = 0$; (b) $t = 600000$; (c) $t = 1200000$; (d) $t = 1800000$; (e) $t = 2400000$; (f) $t = 5000000$.

Finally, increasing d_1 to $d_1 = 9$ and close to Turing bifurcation value, we can find that the spot pattern forms as Figure 3.5 (f).

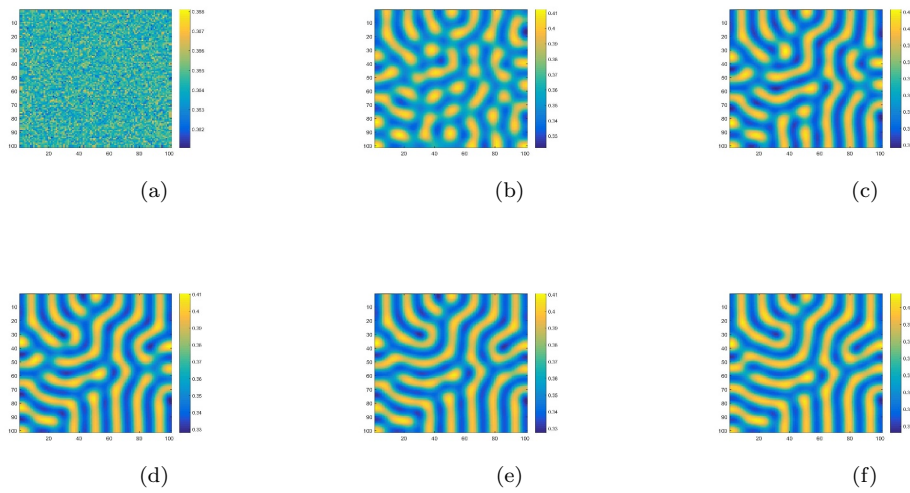


Figure 3.5. Snapshots of contour pictures of the time evolution of the prey population with $\alpha = 0.5$, $\beta = 4$, $\eta = 1$, $d_2 = 0.1$, $\gamma = 0.175$, $d_1 = 9$. (a) $t = 0$; (b) $t = 550000$; (c) $t = 950000$; (d) $t = 2550000$; (e) $t = 4350000$; (f) $t = 5000000$.

In this case, from the figures above, in the plane of $\gamma - d_1$, for fixed $\gamma = 0.175$, the different pattern formations up to the value of the diffusion coefficient of the prey. In other words, as the value of d_1 moves away from Turing bifurcation, we find three patterns: spot pattern, spot-stripe

pattern, and stripe pattern. In particular, if the value is close to Turing bifurcation, the form of the pattern is spot pattern.

4 Conclusion and Discussion

In this paper, we study a kind of predator-predator model with Holling type II functional response and Allee effect in predator. Firstly, this paper theoretically analyzes the existence and stability of the non-negative equilibrium of the system. We mainly explore the influence of the strength (measured by γ) of the Allee effect of the predator on the existence and stability of the coexistence equilibrium (also called positive equilibrium).

For the existence of the coexistence equilibrium, in terms of the relationship of other parameters of the system, the influence of the Allee effect can be divided into two cases: (i) there is no coexistence equilibrium for any $\gamma \geq 0$; (ii) there exists a critical value γ_* of the strength of the Allee effect such that the system has two coexistence equilibria for $0 < \gamma < \gamma_*$ and no coexistence equilibrium for $\gamma > \gamma_*$. This critical value γ_* can be explicitly determined. Notice that the boundary equilibrium $(1, 0)$ (predator extinction equilibrium) is always stable and the per growth rate of predator decreases with the increasing of the strength of the Allee effect. Therefore, the larger Allee effect can lead to the smaller per capital reproduction rate of predator, and when the per reproduction rate is smaller than death rate, the per capital growth rate of the predator will be negative, eventually leading to the extinction of the predator. Thus, for the ecological balance, keeping the moderate Allee effect is necessary. In addition, the Allee effect leads to the appearance of two coexistence equilibria although one is always unstable, which is useful for biological diversity.

For the stability of the two coexistence equilibria, it has been shown that the one corresponding to low predator biomass is always a saddle, and the stability of the other one depends on the strength of the Allee effect and other parameters of the system. In this paper, we focus on how the strength of the Allee effect affects the stability of the coexistence equilibrium corresponding to high predator biomass. Our theoretical results show that there are three kinds of possible cases about the stability: (i) the strength of the Allee effect does not affect the stability of this coexistence equilibrium; (ii) there exists a unique Hopf bifurcation value γ_H^* such that this coexistence equilibrium is asymptotically stable for $0 \leq \gamma < \gamma_H^*$ and unstable for $\gamma_H^* < \gamma < \gamma_*$; (iii) there exists two Hopf bifurcation values $\gamma_H^{(1)}$ and $\gamma_H^{(2)}$ such that the stability switches induced by Allee effect occur, i.e., this coexistence equilibrium is asymptotically stable for $0 \leq \gamma < \gamma_H^{(1)}$ or $\gamma_H^{(2)} < \gamma < \gamma_*$, and unstable for $\gamma_H^{(1)} < \gamma < \gamma_H^{(2)}$. Destabilizing force of Allee effect in predator-prey systems has been known^[4, 18, 34-36, 43]. Here the existence of the stability switches induced by Allee effect has also shown the stabilizing force for relatively large strength of Allee effect. The numerical simulations also shown the existence of the stable periodic orbit bifurcating from these Hopf bifurcations. It is also shown that there exist two kinds of bistabilities: one is the coexistence of stable coexistence equilibrium and stable predator extinction equilibrium and the other is the coexistence of stable periodic orbit and stable predator extinction equilibrium.

Finally, we investigate the diffusion on the influence of diffusion on the stability of the coexistence equilibrium. When there is no Allee effect, there is no diffusion-driven Turing instability for the original predator-prey system. However, when the Allee effect is introduced into the reproduction rate of the predator, there exists diffusion-driven Turing instability for the case when predator spread slower than prey. The Turing bifurcation value is also explicitly determined taking the diffusion coefficient of the prey as the parameter. Numerical simulations has been shown that with the increasing of the diffusion coefficient of the prey, there are three kinds of different patterns: spot pattern, spot-stripe pattern, and stripe pattern.

Conflict of Interest

The authors declare no conflict of interest.

References

- [1] Ackleh, A.S., Allen, L.J.S., Carter, J. Establishing a beachhead: A stochastic population model with an Allee effect applied to species invasion. *Theor. Popul. Biol.*, 71(3): 290–300 (2007)
- [2] Arancibia-Ibarra C., Flores J.D., Pettet G., Heijster P. A Holling-Tanner predator-prey model with strong Allee effect. *Int. J. Bifurc. Chaos.*, 29: 1930032: 1–1930032: 16 (2019)
- [3] Berec L. Impacts of foraging facilitation among predators on predator-prey dynamics. *Bull. Math. Biol.*, 72(1): 94–121 (2010)
- [4] Bodine E.N., Yust A.E. Predator-prey dynamics with intraspecific competition and an Allee effect in the predator population. *Lett. Biomath.*, 4(1): 23–38 (2017)
- [5] Boukal D., Berec L. Single-species models of the Allee effect: Extinction boundaries, sex ratios and mate encounters. *J. Theor. Biol.*, 218(3): 375–394 (2002)
- [6] Boukal D.S., Sabelis M.W., Berec L. How predator functional responses and Allee effects in prey affect the paradox of enrichment and population collapses. *Theor. Popul. Biol.*, 72(1): 136–147 (2007)
- [7] Capone F., Carfora M.F., Luca R.De, Torricollo I. Turing patterns in a reaction-diffusion system modeling hunting cooperation. *Math. Comput. Simul.*, 165(Nov): 172–180 (2019)
- [8] Chang X.Y., Shi J.P., Zhang J.M. Dynamics of a scalar population model with delayed Allee effect. *Int. J. Bifurc. Chaos.*, 28(12): 1850153: 1–1850153: 15 (2018)
- [9] Cheng K.S. Uniqueness of a limit cycle for a predator-prey system. *Siam. J. Math. Anal.*, 12(4): 541–548 (1981)
- [10] González-Olivares, E., Mena-Lorca, J., Roja-Palma, A., Flores, J.D. Dynamical complexities in the Leslie-Gower predator-prey model as consequences of the Allee effect on prey. *Appl. Math. Model.*, 35(1): 366–381 (2011)
- [11] Hsu S.B. On global stability of a predator-prey system. *Math. Biosci.*, 39(1): 0025–5564 (1978)
- [12] Hsu S.B. A survey of constructing lyapunov functions for mathematical models in population biology. *Taiwan. J. Math.*, 9(2): 151–173 (2005)
- [13] Johnson D.M., Liebhold A.M., Tobin P.C., Bjornstad O.N. Allee effects and pulsed invasion by the gypsy moth. *Nature.*, 444(7117): 361–363 (2006)
- [14] Kanarek A.R., Webb C.T., Barfield M., Holt R.D. Allee effects, aggregation, and invasion success. *Theor. Ecol.*, 6(2): 153–164 (2013)
- [15] Kang Y., Udiani O. Dynamics of a single species evolutionary model with Allee effects. *J. Math. Anal. Appl.*, 418(1): 492–515 (2014)
- [16] Kangalgil F. Neimark-sacker bifurcation and stability analysis of a discrete-time prey-predator model with allee effect in prey. *Adv. Differ. Equ.*, 2019(1): 1–12 (2019)
- [17] Kramer A.M., Dennis B., Liebhold A.M., Drake J.M. The evidence for Allee effects. *Popul. Ecol.*, 51(3): 341–354 (2009)
- [18] Lai X.H., Liu S.Q., Lin R.Z. Rich dynamical behaviours for predator-prey model with weak Allee effect. *Appl. Anal.*, 89(8): 1271–1292 (2010)
- [19] Liu P., Yang B. Dynamics analysis of a reaction-diffusion system with Beddington-DeAngelis functional response and strong Allee effect. *Nonlinear Anal.-Real World Appl.*, 51: 102953 (2020).
- [20] Liu X., Fan G.H., Zhang T.H. Evolutionary dynamics of single species model with Allee effect. *Physica A.*, 526: 120774 (2019)
- [21] Liu Y., Ruan S.G., Yang L. Stability transition of persistence and extinction in an avian influenza model with Allee effect and stochasticity. *Commun. Nonlinear Sci. Numer. Simulat.*, 91: 105416 (2020)
- [22] Liu Y.Y., Wei J.J. Spatiotemporal dynamics of a modified Leslie-Gower model with weak Allee effect. *Int. J. Bifurc. Chaos.*, 30(12): 2050169 (2020)
- [23] Liu Y.W., Zhang T.H., Liu X. Investigating the interactions between Allee effect and harvesting behaviour of a single species model: An evolutionary dynamics approach. *Physica A.*, 549: 124323 (2020)
- [24] Mandal P.S., Kumar U., Garain K., Sharma R. Allee effect can simplify the dynamics of a prey-predator model. *J. Appl. Math. Comput.*, 63(1-2): 739–770 (2020)
- [25] Murray J. *Mathematical Biology II: Spatial Models and Biomedical Application.* Springer, 1993
- [26] Roos A.de, Persson L., Thieme H.R. Emergent Allee effects in top predators feeding on structured prey populations. *Proc. R. Soc. B-Biol. Sci.*, 270(1515): 611–618 (2003)
- [27] Sen D., Ghorai S., Banerjee M. Allee effect in prey versus hunting cooperation on predator-enhancement of stable coexistence. *Int. J. Bifurc. Chaos.*, 29(6): 1950081 (2019)
- [28] Sen D., Petrovskii S., Ghorai S., Banerjee M. Rich bifurcation structure of prey-predator model induced by the Allee effect in the growth of generalist predator. *Int. J. Bifurc. Chaos.*, 30(6): 2050084 (2020)

- [29] Sen M., Banerjee M., Morozov A. Bifurcation analysis of a ratio-dependent prey-predator model with the Allee effect. *Ecol. Complex.*, 11(SEP): 12–27 (2012)
- [30] Song D.X., Song Y.L., Li C. Stability and Turing patterns in a predator-prey model with hunting cooperation and Allee effect in prey population. *Int. J. Bifurc. Chaos.*, 30(9): 2050137 (2020)
- [31] Stephens P.A., Sutherland W.J. Consequences of the allee effect for behaviour, ecology and conservation. *Trends. Ecol. Evol.*, 14(10): 401–405 (1999)
- [32] Sun G.Q. Mathematical modeling of population dynamics with Allee effect. *Nonlinear Dyn.*, 85(1): 1–12 (2016)
- [33] Teixeira Alves, M., Hilker F.M. Hunting cooperation and Allee effects in predators. *J. Theor. Biol.*, 419: 13–22 (2017)
- [34] Terry A.J. Predator-prey models with component Allee effect for predator reproduction. *J. Math. Biol.*, 71(6-7): 1325–1352 (2015)
- [35] Tyutyunov Y.V., Sen D., Titova L.I., Banerjee M. Predator overcomes the Allee effect due to indirect prey-taxis. *Ecol. Complex.*, 39: 100772 (2019)
- [36] Verdy A. Modulation of predator-prey interactions by the Allee effect. *Ecol. Model.*, 221(8): 1098–1107 (2010)
- [37] Wang J.F., Shi J.P., Wei J.J. Dynamics and pattern formation in a diffusive predator-prey system with strong Allee effect in prey. *J. Differ. Equ.*, 251(4-5): 1276–1304 (2011)
- [38] Wang X.Q., Cai Y.L., Ma H. Dynamics of a Diffusive Predator-Prey Model with Allee Effect on Predator. *Discrete Dyn. Mat. Soc.*, 2013: 1–10 (2013)
- [39] Wei Z.X., Xia Y.H., Zhang T.H. Stability and Bifurcation Analysis of an Amensalism Model with Weak Allee Effect. *Qual. Theor. Dyn. Syst.*, 19(1): 1–15 (2020)
- [40] Wu D.Y., Zhao H.Y. Spatiotemporal dynamics of a diffusive predator-prey system with Allee effect and threshold hunting. *J. Nonlinear Sci.*, 30(3): 1015–1054 (2019)
- [41] Yi F.Q., Wei J.J., Shi J.P. Bifurcation and spatiotemporal patterns in a homogeneous diffusive predator-prey system. *J. Differ. Equ.*, 246(5): 1944–1977 (2009)
- [42] Zhang C.H., Yang W.B. Dynamic behaviors of a predator-prey model with weak additive Allee effect on prey. *Nonlinear Anal.-Real World Appl.*, 55: 103137 (2020)
- [43] Zhou S.R., Liu Y.F., Wang G. The stability of predator-prey systems subject to the allee effects. *Theor. Popul. Biol.*, 67(1): 23–31 (2005)
- [44] Zu J., Mimura M. The impact of Allee effect on a predator-prey system with Holling type II functional response. *Appl. Math. Comput.*, 217(7): 3542–3556 (2010)
- [45] Zuo W.J., Song Y.L. Stability and double-hopf bifurcations of a Gause-Kolmogorov-type predator-prey system with indirect prey-taxis. *J. Dyn. Differ. Equ.*, 33(4): 1917–1957 (2021)